ELSEVIER

Journal of Alloys and Compounds 394 (2005) 160–167

Journal of ALLOYS AND COMPOUNDS

www.elsevier.com/locate/jallcom

Microwave activated combustion synthesis of bulk cobalt silicides

J.R. Jokisaari, S. Bhaduri, S.B. Bhaduri*

School of Materials Science and Engineering, Clemson University, Clemson, SC 29634, USA

Received 14 July 2004; received in revised form 19 October 2004; accepted 19 October 2004
Available online 8 December 2004

Abstract

CoSi and $CoSi_2$ bulk intermetallic compounds have generated some interest as potential electronic and structural materials. Combustion synthesis has been shown to be an effective method for the preparation of many intermetallic compounds, but requires a high adiabatic temperature to propagate. Thermodynamic calculations show that cobalt silicides require activation. Microwave activation is attractive for combustion synthesis reactions, allowing rapid heating and cooling rates, volumetric heating, and direct absorption of energy by the reaction zone. In this study, a microwave activated combustion synthesis process was used to produce CoSi and $CoSi_2$ bulk cobalt silicides. Thermal activation and conventional combustion synthesis were also attempted, and the results of the three processes are compared.

Keywords: Intermetallic compounds; Combustion; Microwave activation

1. Introduction

Over the last decade, transition metal silicides have gained considerable attention as potential materials for both structural and electronic applications. They have a high thermal stability, corrosion resistance, favorable mechanical properties, and a low electronic sheet resistance that makes them suitable for electronic applications. They have been extensively researched in thin film form for .25 μm and below CMOS electronics [1–6]. In addition, cobalt silicide has been investigated for use as a solid catalyst for the formation of carbon nanotubes [7], and in silicon carbide composites for structural applications [8].

Bulk $CoSi_2$ is required for use as a source for the production of thin films in sputtering processes. Sputtering targets are generally processed either by a powder route, casting or mechanical working means. Like other silicides, cobalt silicides, being brittle materials, suffer processing-related difficulties. Combustion synthesis is an alternate and well-proven technique to produce silicides [9–11]. The process is based on the principle that an exothermic reaction may be triggered by an external heat source, resulting in a self-sustaining exothermic reaction that yields products without application of further external heat [12]. This process is considerably faster than conventional processes (milliseconds to seconds as opposed to several hours for conventional methods), and is generally more energy efficient. From a thermodynamic viewpoint, combustion requires a reaction with high negative enthalpy (ΔH_{rxn}) and moderate to high adiabatic temperature (T_{ad}) [11]. Using the adiabatic temperature is a simplifying assumption. While adiabatic conditions are not always maintained, calculating T_{ad} serves as a guideline for assessing the potential of using a CS reaction for synthesis of advanced materials.

However, in many cases reactions are not exothermic enough to be self-sustaining. In these systems the propagation of reaction fronts is erratic and non-uniform [11]. This leads to non-uniform microstructures and properties. Many reactions belong in this category, including cobalt silicides. Several strategies exist for activation. These include the application of thermal [13], mechanical [14,15], or electromagnetic energy [16–20]. Pre-heating, or thermally activated combustion synthesis (TACS), is one of the simplest and more widely used strategies for activation of CS reactions. TACS processes have been shown to be highly sensitive to heating rate [13]. This is a drawback as most furnaces are limited to relatively low heating and cooling rates (10’s of de-

---

* Corresponding author. Tel.: +1 864 656 3176; fax: +1 864 656 5973.
E-mail address: bhaduri@clemson.edu (S.B. Bhaduri).

0925-8388/$ – see front matter © 2004 Elsevier B.V. All rights reserved.
doi:10.1016/j.jallcom.2004.10.024

grees/minute) determined by the furnace cycle, which leaves ample time for diffusion and formation of undesirable phases during processing [13]. Maglia et al. describe an electromagnetic activation method for combustion synthesis reactions, field activated combustion synthesis (FACS), in vanadium, tantalum, and tungsten silicides [18–20]. FACS shares some similarities with MACS. In FACS, an appropriately shaped sample is placed between two electrodes and a voltage is applied. A tungsten coil is used to initiate the reaction. The electric field provides energy to the propagating reaction. The tungsten coil in FACS plays a similar role to the susceptor in MACS, excepting the susceptor also provides pre-heating and, if desired, continued post-combustion heating. The processes differ in the method of application of the electric field. FACS utilizes a mechanism of joule heating due to electrical resistance, while MACS relies on the dielectric properties of the material.

Electromagnetic activation via microwave has some interesting consequences due to the manner in which the energy is absorbed. Microwave energy is absorbed volumetrically, resulting in volumetric heating [21,22]. The heated area is limited to the sample volume and the susceptor (if one is used). This inverts the temperature profile, with the surface of the sample being cooler than the interior. Heat generation at the sample and the inverted temperature profile allow for very rapid heating and cooling rates [17–19]. Once the reaction begins, the hot reaction zone becomes the most strongly absorbing area in the system. This is due to the rise in dielectric loss factor that occurs as the temperature is raised [23]. Above a certain threshold, the absorption of microwaves by the sample rises very rapidly [22,23]. This condition, generally referred to as thermal runaway, is a unique effect of microwave activated processing. This effect also aids in CS processing of high-density green bodies, which is difficult by other methods [22]. In addition, microwave energy has been shown to reduce the apparent activation energy of a reaction [22,24]. This phenomenon has been documented in catalyzed reactions [24], and in terms of enhanced diffusion during sintering [25].

The first objective of the current paper was to explore a ‘Microwave Activated Combustion Synthesis (MACS)’ process in order to synthesize $CoSi_2$ and CoSi. From the thermodynamic data, we have found that adiabatic temperature for $CoSi_2$ is not high enough for the compound formation in CoSi binary system to propagate and therefore activation was required. The second objective was to compare the MACS process with other variants of the combustion synthesis process (e.g. thermal activation in a furnace and conventional CS). The products of the processes were characterized by XRD and SEM, and compared.

2. Experimental procedure

Elemental cobalt (99.9%, <5 μm) and silicon (99.5%, −325 mesh) were procured from Aldrich Chemicals. The two constituents were mixed at the stoichiometric ratio containing 32.3 wt.% Si for CoSi and 48.8 wt.% Si for $CoSi_2$, respectively. The powders were ball milled for 2 h to ensure homogeneous mixing. Pellets were first uniaxially pressed in a cylindrical metal die, then cold isostatically pressed at 100 MPa to produce green billets. Uniaxial pressing prior to CIPing provides a better surface finish than CIPing alone, while the CIP produces higher green density and more readily handled pellets. The final cylindrical pellets were nominally 13 mm in diameter and 10 mm tall. After pressing, the

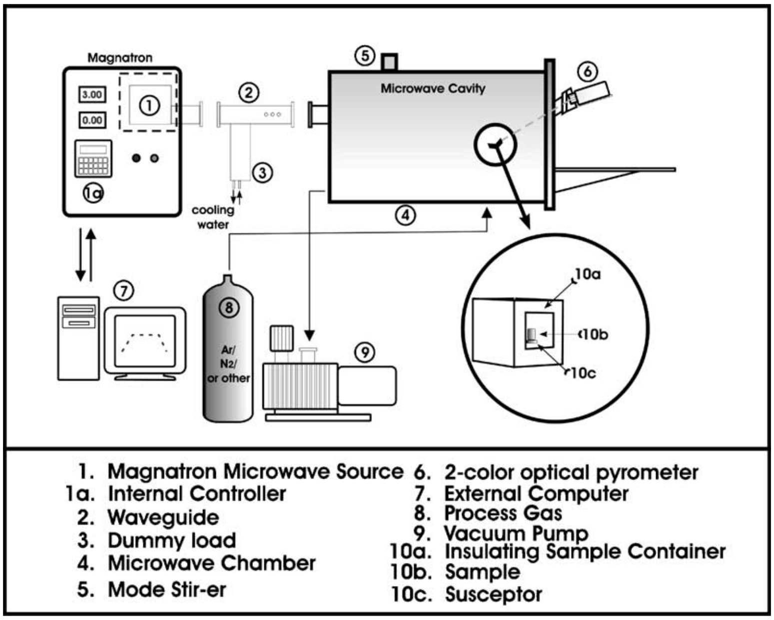

Fig. 1. Schematic diagram of microwave system setup.

samples were degassed in a high purity argon atmosphere at 600 °C/4 h (2 h soaking) to remove any absorbed moisture and low temperature impurities.

For MACS, samples were placed in an Al_2O_3 fiberboard container (Zircar Al-30), and surrounded with alumina fiber insulation. The alumina fiber and board is insulating, but not significantly absorbing at the operating frequency. A SiC disc susceptor 2.54 cm in diameter and .75 cm tall placed under the sample was used to provide pre-heating. Temperature measurements were made using a two color optical pyrometer (Mikron, NJ, model M77LS, temperature range: 1000–3000 °C). The pyrometer was set about 35 cm away from the sample and aligned with 2 cm diameter quartz view port located on the front door of the MW chamber. The measured spot on the surface of the sample was approximately 2 mm at the center of the cylindrical sample. The samples were then ignited in the industrial microwave furnace (MMT, Knoxville, TN). The MMT system is provided with a variable power output magnetron source capable of operating from 0 to 3 kW at 2.45 GHz. The cavity is large and ‘overmoded’, ensuring mixing of the microwave modes and resulting in a homogeneous field distribution. A video camera was used to monitor the reaction propagation through an electrically shielded port. The system schematic is given in Fig. 1.

Conventional CS was carried out in a steel reaction chamber, which was evacuated and backfilled with high purity argon. The sample was placed on a graphite stage and triggered from the top using a tungsten coil. A video camera was used to monitor the reaction propagation through a quartz window. Thermally activated samples were reaction sintered in a furnace (Centorr Associates) at 1200 °C for 4 h under argon.

X-ray diffraction patterns of the product were recorded by a Siemens diffractometer (D5000) using Cu Kα radiation at 40 kV and 30 mA. The microstructures of the as-polished and as-etched samples were examined via a scanning electron microscope (SEM model AMRAY 1830) equipped with an energy dispersive X-ray analyzer.

3. Results and discussion

3.1. Thermodynamics

The parameters governing any combustion synthesis process are largely determined by the energy released. Assuming adiabatic conditions, the parameter T_{ad} is a convenient and commonly cited parameter to characterize these processes. A T_{ad} of 1800 K is suggested in the literature to determine if a given reaction will be self-sustaining and the mode of propagation [11,12]. The adiabatic temperature is calculated from heating of the product from 298 K to T_{ad} in response to the input of $H_{reaction}$ (Eq. (1)). Since in CoSi, T_{ad} of the product calculated by the first method exceeds the melting temperature, the enthalpy of melting of the product must also be taken into consideration resulting in Eq. (2):

$$-\Delta H_{f,298} = \int_{298}^{T_{ad}} C_{p(\text{product})}\,dT \tag{1}$$

$$\begin{aligned} -\Delta H_{f,298} &= \int_{298}^{T_{mp}} Cp(\text{product})\,dT + \Delta H_m \\ &\quad + \int_{T_{mp}}^{T_{ad}} Cp(\text{liquid})\,dT \end{aligned} \tag{2}$$

Table 1 gives calculated T_{ad} values for CoSi and $CoSi_2$.

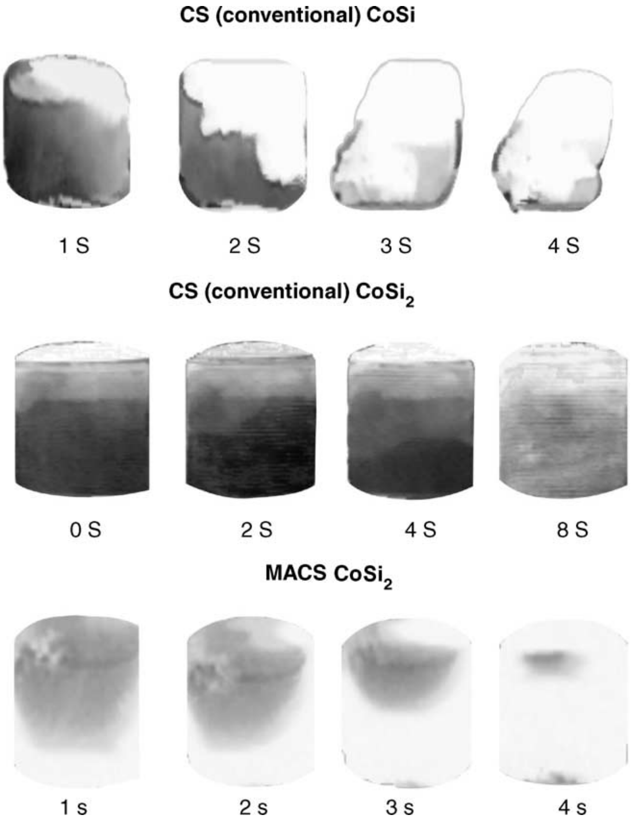

Fig. 2. Captured video of reaction propagation in CoSi and $CoSi_2$ in MACS and conventional CS processes. The video for CoSi is from conventional CS, as the same behavior was observed in MACS. However, in $CoSi_2$, there is a change in the manner of propagation from lower-energy spin mode to planar propagation.

Table 1
Thermodynamic data and calculated T_{ad} values for cobalt silicides

Compound	A (J mol^{-1} K^{-1})	$B \times 10^{-3}$ (J mol^{-1} K^{-2})	$C \times 10^{5}$ (J mol^{-1} K)	ΔH_f (kJ mol^{-1})	ΔH_m (kJ mol^{-1})	T_m (K)	T_{ad} (K)
$CoSi_2$	70.857	18.661	−9.918	−102.93	60.75	1599	1527
CoSi	49.166	12.090	−7.537	−95.04	57.00	1733	1732

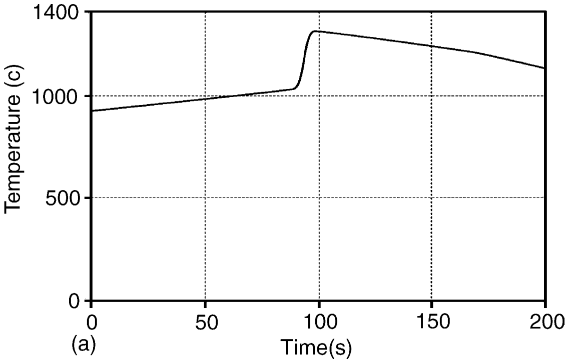

Fig. 3. Heating profile for CoSi in MACS.

For many compounds, the thermodynamic data required to calculate T_{ad} are available in the literature. The heat capacity (in $J\,mol^{-1}\,K^{-1}$) is written as $a + bT + c/T^2$, where the coefficients a, b and c and $\Delta H_{f,298}$ values were obtained from the HSC^{TM} thermodynamic software package (V 4.1, Outokumpu, Finland).

The adiabatic temperature calculated for $CoSi_2$ falls well below the 1800 K required for self-propagation [11,22]. T_{ad} for CoSi is rather close to that limit. Based on these results, CoSi may be expected to form under conventional CS, while $CoSi_2$ would not.

In the MACS process, there are a number of other factors that affect the reaction. Microwave energy is absorbed volumetrically, so heating occurs simultaneously throughout the sample [21,22]. The heated area is limited to the sample volume and the susceptor (if one is used). Additionally, once the reaction begins, the hot reaction zone becomes the most strongly absorbing area of the system. This is due to the rise in dielectric loss factor that occurs as the temperature rises above a particular threshold [23]. This allows for very rapid heating and cooling rates and can reduce the apparent activation energy of a reaction [22,24]. The effect of microwave activation was expected to be enhanced reaction kinetics, more rapid propagation, and a more pure product. Our results showed that, while a reaction will propagate for both CoSi and $CoSi_2$ under all three methods attempted, the mode of propagation differed in response to the manner of activation in $CoSi_2$. The reaction propagation occurred in spin mode in conventional CS, most likely volume explosion mode in TACS, and was planar in MACS. Successful propagation in CoSi was expected for all three processing routes. This

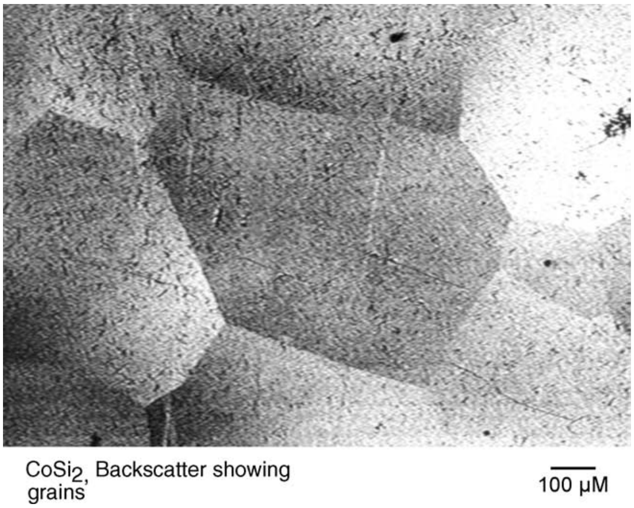

Fig. 4. SEM of dense $CoSi_2$. The very large grains are likely the result of partial melting of the product coupled with grain growth from sintering very near the melting point.

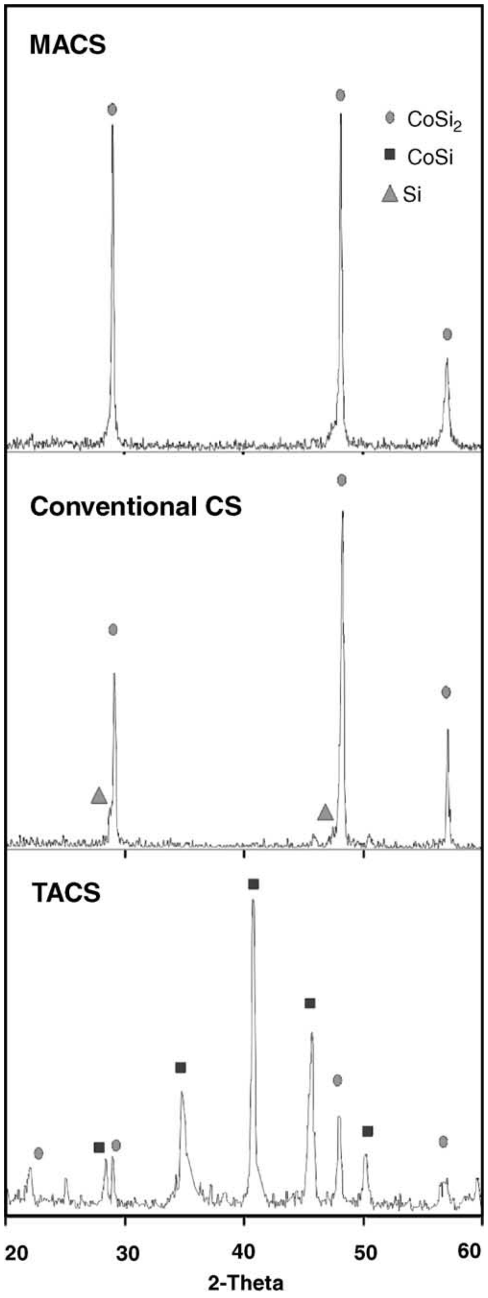

Fig. 5. XRD data comparing $CoSi_2$ obtained from each processing route. The product of the MACS route was pure $CoSi_2$, while conventional CS shows the presence of residual silicon, and TACS contains a mixture of both $CoSi_2$ and CoSi.

agrees well with expectations based on the thermodynamic considerations.

3.2. $CoSi_2$

$CoSi_2$ behaves in a significantly different manner under MACS than in conventional CS. Captured video frames of the reaction in progress are shown in Fig. 2. Under MACS, reaction propagation is apparently planar. This corresponds to a higher energy mode of propagation than would be expected given the adiabatic temperature. The temperature profile in Fig. 3 shows the reaction in $CoSi_2$. The ignition temperature was approximately 1273 K, with a peak temperature of 1623 K. This is well above the theoretical adiabatic temperature and the melting temperature of the product. However, though partial melting is evident in the microstructure, the bulk of the sample did not melt. This was most likely due to rapid cooling by radiation to the surroundings. When removed from the furnace immediately, the microstructure of $CoSi_2$ was relatively uniform and porous. If the power was left on after the reaction was complete, the sample continued to sinter and approached full density after a total processing time of approximately 20 min. This post-reaction sintering in situ densified the material, but resulted in massive grain growth. SEM of synthesized samples, shown in Fig. 4, shows grains in excess of 300 μm in diameter.

XRD of $CoSi_2$ produced by each of the processes is given in Fig. 5. Fully dense $CoSi_2$ samples appear to contain two phases. Both the dark and light regions appear to be $CoSi_2$ in composition, with a slight excess of silicon in the darker regions, as shown in the EDAX data in Fig. 6. This does not appear in the XRD patterns, and therefore the dark phase is likely amorphous. It is interesting to note that while the phase

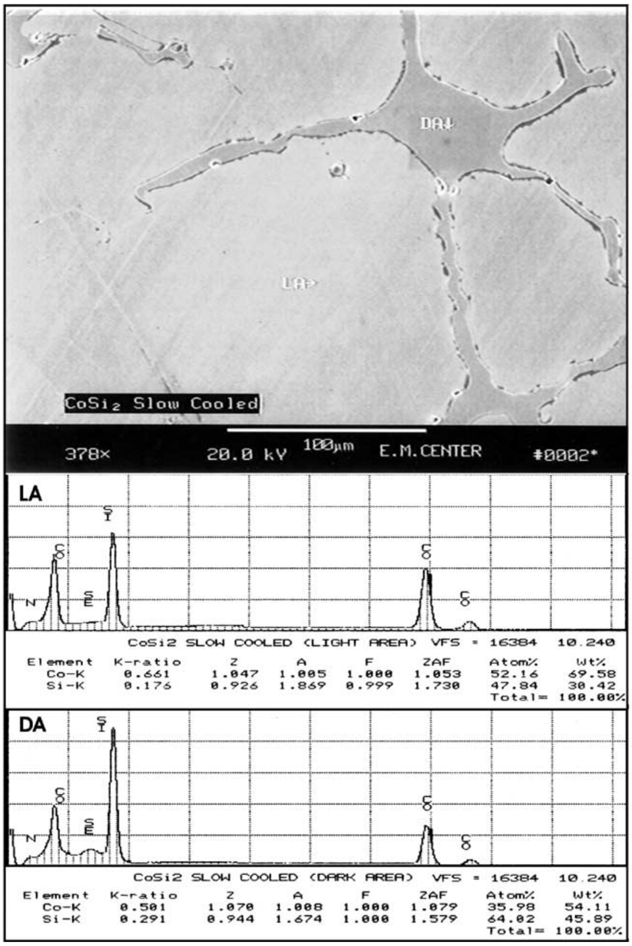

```
                CoSi2 SLOW COOLED (LIGHT AREA)  VFS = 16384   10.240
 Element   K-ratio       Z       A       F      ZAF      Atom%      Wt%
   Co-K     0.661     1.047   1.005   1.000   1.053     52.16     69.58
   Si-K     0.176     0.926   1.869   0.999   1.730     47.84     30.42
                                                        Total=  100.00%
```

```
                CoSi2 SLOW COOLED (DARK AREA)   VFS = 16384   10.240
 Element   K-ratio       Z       A       F      ZAF      Atom%      Wt%
   Co-K     0.501     1.070   1.008   1.000   1.079     35.98     54.11
   Si-K     0.291     0.944   1.674   1.000   1.579     64.02     45.89
                                                        Total=  100.00%
```

Fig. 6. SEM of $CoSi_2$ showing the presence of a second phase in the grain boundary near the edge of the sample. The dark phase appears to be silicon-rich under EDAX. As it does not appear under XRD, it is most likely amorphous.

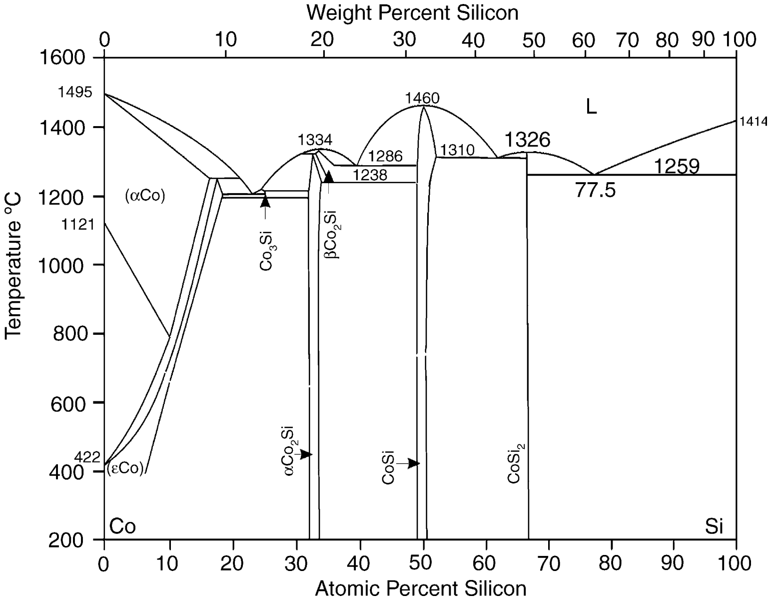

Fig. 7. Phase diagram for the CoSi system. CoSi exists over a range of composition, and altering the composition may be one method of preventing the formation of $CoSi_2$ precipitates in the reaction product. $CoSi_2$ appears as a line compound [26].

diagram for the system shows CoSi to cover a broad range of compositions and $CoSi_2$ to be a line compound (Fig. 7, [26]), it was easy to obtain $CoSi_2$, but CoSi was always accompanied by precipitates of $CoSi_2$.

$CoSi_2$ produced in TACS did not densify, and easily crumbled into powder. This could be explained if the reaction occurred at many points simultaneously rather than in a well-organized reaction wave. XRD analysis of the powder revealed a mixture of both CoSi and $CoSi_2$ (Fig. 5) formed, with CoSi being the major phase. The heating rate sensitivity of CS processes can be used to explain this result. Thermal activation provides the lowest heating rate to ignition of the three processes compared here. This allows time for pre-ignition reactions to define the product [13] as the more energetic CoSi reaction appears to occur at lower temperature than that of the $CoSi_2$ reaction. This is consistent with the much higher ignition temperature noted for $CoSi_2$ in the MACS process.

In conventional combustion synthesis, the CS reaction was not expected to propagate for $CoSi_2$. In actuality, while the reaction did propagate, it did so in ‘spin’ mode, which is associated with sluggish propagation [11]. Fig. 2 shows several successive frames of captured video from this reaction. The reaction was initiated close to the tungsten coil and propagated in a spiral fashion down the sample. The front of the spiral wave appeared rough as well. This mode of propagation has been shown to result in incomplete conversion and an inhomogeneous product [11]. XRD of samples produced by conventional CS shows the presence of some residual silicon, but does not contain appreciable CoSi. Both conventional CS and MACS utilize a high heating rate up to ignition, followed by rapid cooling. This prevented the formation of CoSi before $CoSi_2$ in conventional CS, compared to TACS. The presence of residual silicon was most likely the result of incomplete reaction due to the spin mode propagation. Conventional CS product samples had a banded structure, with dense bands alternating with porous ones corresponding to the progress of the reaction wave.

3.3. CoSi

Fig. 8 is of the temperature profile for CoSi in the MACS process. The sample was completely melted as the combustion wave progressed. Ignition occured as soon as the temperature rose above 950 °C. The temperature peaked at approximately 1798 K, above the melting point of the material and somewhat above the theoretical adiabatic temperature. This is due to both coupling of the microwaves within the sample, as well as pre-heating by the susceptor. The rapid fall of the peak can be attributed to resolidification of the sample after the passage of the combustion wave. On examination by SEM, precipitates of $CoSi_2$ appear in CoSi samples (Fig. 9). There are also a few nodules of silicon dispersed in the microstructure, primarily at the grain boundaries. XRD was only able to identify CoSi in the product (Fig. 10). TACS yielded a melted droplet, similar to MACS and conventional processing. It had a slightly higher porosity and grain size than samples produced by the other routes.

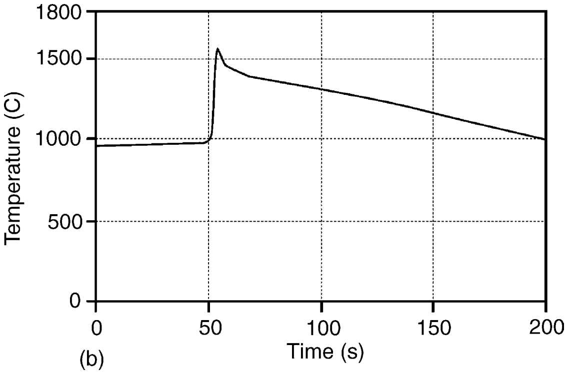

Fig. 8. Heating profile for $CoSi_2$ in MACS.

CoSi could be successfully produced by conventional CS. As the adiabatic temperature exceeds the melting temperature of this material, the sample melted, producing a droplet

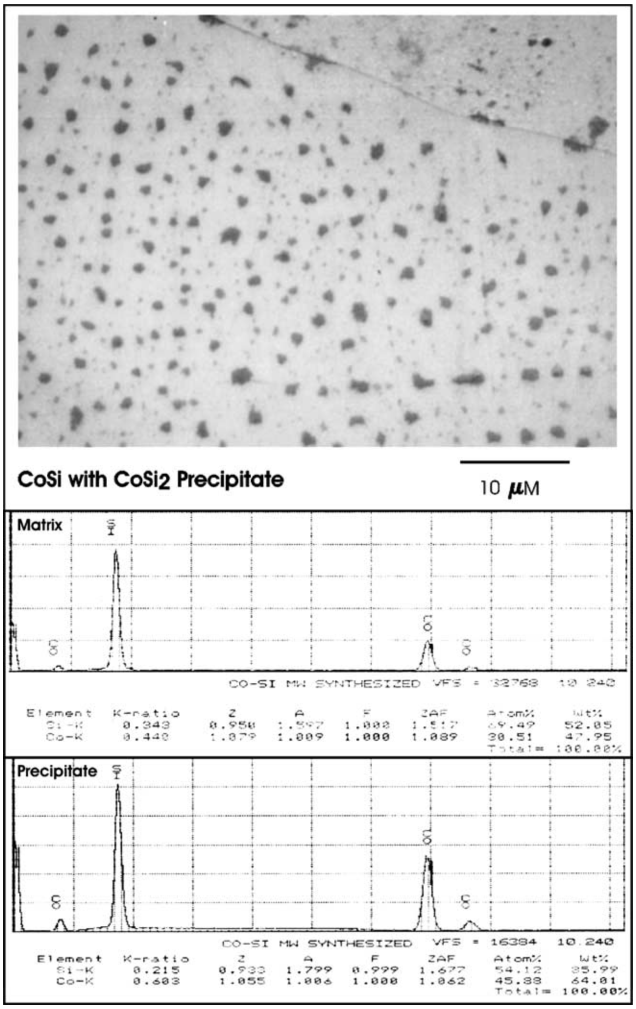

```
                        CO-SI MW SYNTHESIZED  VFS = 32768   10.240

 Element  K-ratio      Z      A      F      ZAF     Atom%     Wt%
   Si-K    0.343    0.950  1.597  1.000  1.517   69.49    52.05
   Co-K    0.440    1.079  1.009  1.000  1.089   30.51    47.95
                                                 Total=  100.00%
```

```
                        CO-SI MW SYNTHESIZED  VFS = 16384   10.240
 Element  K-ratio      Z      A      F      ZAF     Atom%     Wt%
   Si-K    0.215    0.933  1.799  0.999  1.677   54.12    35.99
   Co-K    0.603    1.055  1.006  1.000  1.062   45.88    64.01
                                                 Total=  100.00%
```

Fig. 9. SEM of CoSi by MACS, showing precipitates formed with slight aging. EDAX identifies these precipitates as $CoSi_2$. Similar results were obtained from all processing routes.

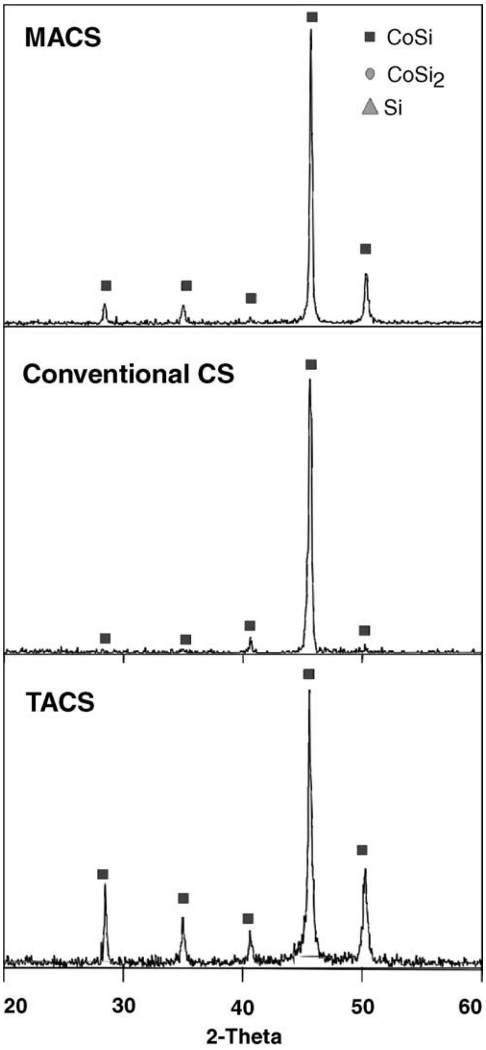

Fig. 10. XRD data comparing CoSi from each of the three processing routes. The product of each route was similar.

similar to those of the MACS and TACS processes. XRD results from these samples were quite similar to those of the MACS process. Both conventional CS and MACS utilize much higher heating rates than TACS as presented here. The high heating rates may reduce the occurrence of undesired reactions, and the opportunity for grain growth. This may explain the difference in material produced via the CS, MACS, and TACS routes.

CoSi was successfully produced by all three processing routes. Some differences in the final phase were noted in the XRD patterns. In all CoSi reactions, the sample melted completely. In addition, the precipitation of $CoSi_2$ in the CoSi produced by all three methods was noted after some time.

4. Conclusions

While CoSi behaved much the same in synthesis by MACS, conventional CS, and TACS methods, combustion synthesis of $CoSi_2$ proceeded differently. In terms of activation, these results compare well with predictions based on the thermodynamic calculations and literature. Conventional CS occurred in low-energy spin-mode propagation. The result was a banded microstructure and incomplete conversion into product. In TACS, the reaction product was an approximate 50:50 mixture of CoSi and $CoSi_2$, and failed to consolidate. The reaction most likely occurred in thermal explosion mode. This is suggested by the poor consolidation of the product. With MACS, the reaction propagated in a planar manner producing a uniformly porous product of single-phase $CoSi_2$. This could be further sintered in 20 min to near full density, though this sintering resulted in massive grain growth and the appearance of a second, silicon rich, apparently amorphous, phase at the grain boundary. The MACS process is a rapid, effective means of producing substantially single-phase cobalt silicides.

Acknowledgement

This work is partially supported by a NSF grant.

References

[1] K. Maex, Mat. Sci. Eng. Rep. R11 (1993) 53.
[2] R.T. Tung, S. Ohmi, Thin Solid Films 369 (2000) 233.
[3] J.A. Kittl, Q.Z. Hong, Thin Solid Films 320 (1998) 110.
[4] J.A. Kittl, Q.Z. Hong, H. Yang, N. Yu, M.A. Samavedam, M.A. Gribelyuk, Thin Solid Films 332 (1998) 404.
[5] K. Maex, A. Lauwers, P. Besser, E. Kondoh, M. de Potter, A. Steegen, IEEE Trans. Electron. Dev. 46 (1999) 1545.
[6] H.L. Chang, C.H. Lin, C.T. Kuo, Thin Solid Films 420–421 (2002) 219.
[7] K. Inoue, K. Mikagi, H. Abiko, T. Kikkawa, IEDM Tech. Digest 95.
[8] Y. Pan, J.L. Baptista, J. Eur. Cer. Soc. 18 (1998) 201.
[9] R. Radhakrishnan, S.B. Bhaduri, C.H. Henager Jr., JOM 49 (1997) 41.
[10] J.J. Petrovic, MRS Bull. 18 (1993) 35.
[11] S.B. Bhaduri, R. Radhakrishnan, Z.B. Qian, Scripta Met. Mater. 29 (1993) 1089.
[12] Z.A. Munir, U. Anselmi-Tamburini, Mater. Sci. Eng. Rep. R3 (1989) 277.
[13] A. Biswas, S.K. Roy, K.R. Gurumurthy, N. Prabhu, S. Banerjee, Acta Mater. 50 (2002) 757.
[14] B.K. Yen, T. Aizawa, J. Kihara, N. Sakakibara, Mater. Sci. Eng. A 239–240 (1997) 515.
[15] N.N. Thadhani, J. Appl. Phys. 76 (1994) 2129.
[16] Z.A. Munir, Mater. Sci. Eng. A 287 (2000) 125.
[17] J.R. Jokisaari, S. Bhaduri, S.B. Bhaduri, Mater. Sci. Eng. A 323 (2002) 478.
[18] F. Maglia, U. Anselmi-Tamburini, N. Bertolino, C. Milanese, Z.A. Munir, J. Mater. Res. 16 (2001) 534.
[19] F. Maglia, U. Anselmi-Tamburini, C. Milanese, N. Bertolino, Z.A. Munir, J. Alloys Compd. 319 (2001) 108.
[20] L.J. Shon, D.H. Rho, J.C. Kim, Z.A. Munir, J. Alloys Compd. 322 (2001) 120.
[21] A.G. Whittaker, D.M.P. Mingos, J. Microwave Power Electromagn. Energy 29 (1994) 195.
[22] I. Ahmad, R. Dalton, D. Clark, J. Microwave Power Electromagn. Energy 26 (1991) 128.

[23] V.M. Kenkre, L. Skala, M.W. Weiser, J. Mater. Sci. 26 (1991) 2483.
[24] X. Zhang, D.O. Hayward, D.M.P. Mingos, Catal. Lett. 88 (2003) 33.
[25] J.D. Katz, Annu. Rev. Mater. Sci. 22 (1992) 153.
[26] T.B. Massalaski (Ed.), Binary Alloy Phase Diagrams, 2nd ed., The ASM International, Metals Park, OH, 1986.